

Two-, Three-, and Four-Atom Exchange Effects in bcc ^3He

J. H. Hetherington and F. D. C. Willard

Physics Department, Michigan State University, East Lansing, Michigan 48824

(Received 22 September 1975)

We have made mean-field calculations with a Hamiltonian obtained from two-, three-, and four-atom exchange in bcc solid ^3He . We are able to fit the high-temperature experiments as well as the phase diagram of Kummer *et al.* at low temperatures. We find two kinds of antiferromagnetic phases as suggested by Kummer's experiments.

We have been able both to fit the high-temperature solid- ^3He magnetic data¹⁻⁶ and, through mean-field theory, to obtain a phase diagram like that of Kummer *et al.*^{7,8} We consider only three mechanisms of exchange,⁹⁻¹¹ two-atom, three-atom rings, and four-atom rings, and adjust their strengths to fit the data.

The Hamiltonian we take is of the form¹²

$$\mathcal{H} = -\frac{1}{4} \sum_i \sum_\nu J_\nu \vec{\sigma}_i \cdot \vec{\sigma}_{i+\nu} - \mu \vec{B} \cdot \sum_i \vec{\sigma}_i - \frac{1}{4} \sum_{ijkl} \Lambda_{ijkl} (\vec{\sigma}_i \cdot \vec{\sigma}_j) (\vec{\sigma}_k \cdot \vec{\sigma}_l), \quad (1)$$

where the sum over ν indicates a sum over the neighbors of site i . The σ 's are Pauli spin matrices. Ordinary two-atom exchange contributes negatively to J_1 . Three-atom-ring exchange contributes positively to J_1 and J_2 . Four-atom-ring exchanges are of two kinds because there are two kinds of closed four-atom circuits with nearest-neighbor steps. One is folded (F) so that both pairs of opposite corners of the quadrilateral are second neighbors. The second kind is planar (P) diamond shaped so that ends of one diagonal are second neighbors and ends of the other diagonal are third neighbors. We have made calculations using both kinds of four-atom rings but we are able to fit the data using only the F-ring exchanges. The F-ring exchanges contribute negatively to J_1 and J_2 and to two kinds of $(\vec{\sigma}_1 \cdot \vec{\sigma}_2)(\vec{\sigma}_3 \cdot \vec{\sigma}_4)$ terms (" σ^4 "), one where the dot products are between first neighbors and one where they are between second neighbors.

We solved the mean-field equations on the assumption that one of two antiferromagnetic states could exist: (i) the normal (spin-flop) antiferromagnetic (naf) phase, where the two simple cubic sublattices are the magnetic sublattices; and (ii) the simple cubic antiferromagnetic (scf) phase, where each of the simple cubic sublattices is itself antiferromagnetic. The spins on the simple cubic sublattices are rotated 90° about \vec{B} with respect to each other because this minimizes the nearest-neighbor σ^4 term, which en-

ters \mathcal{H} with an overall positive sign.

Without the σ^4 terms in \mathcal{H} only these two structures are possible in mean-field theory when only J_1 and J_2 are nonzero. Without proof, we have assumed that consideration of these two phases is adequate even when the σ^4 terms are present.

The computation proceeded by examining at each value of T and B all solutions of the mean-field equations for the scf, naf, and paramagnetic phases and choosing the solution with lowest free energy.

The high-temperature experiments can be summarized by noting that the partition function Z can be expressed in general in the form¹³

$$N^{-1} \ln Z = \ln 2 + \frac{1}{3} e_2 \beta^2 + \dots + \frac{1}{2} y^2 (1 + \frac{1}{2} \alpha_1 \beta + \dots) + \dots, \quad (2)$$

where $y = \mu B \beta$. We note that specific heat at high T determines e_2 and Curie-Weiss θ determines α_1 . Pressure experiments at zero field determine de_2/dV and have been used to determine e_2 by integration.^{1,2} Pressure experiments in magnetic field¹⁴ measure $d\alpha_1/dV$ and, although somewhat self-contradictory,¹⁵ probably imply on integration an α_1 somewhat smaller than is generally accepted.¹⁶ We can express the results of all high- T experiments (adjusted to $24.2 \text{ cm}^3/\text{mole}$) by the statements that $e_2 = 6.94 \pm 0.3 \text{ (mK)}^2$ mainly on the basis of the results of Panczyk and Adams² and that $\alpha_1 = -6.25 \pm 0.8 \text{ mK}$ mainly from Kirk, Osgood, and Garber.⁵

The theoretical expansions are $\alpha_1 = 8J_1 + 6J_2$ and $e_2 = 12J_1^2 + 9J_2^2 + 31.5K_4^2$, where J_1 and J_2 are usual first- and second-neighbor exchange coefficients and K_4 is the strength of the σ^4 term in the F-ring exchange. K_4 is defined so that the first- and second-neighbor exchange parts of the Hamiltonian due to F-ring exchange alone are $J_1 = 3K_4$ and $J_2 = 2K_4$.

Our fit is obtained with $J_1 = -0.56 \text{ mK}$, $J_2 = 0.175 \text{ mK}$, and $K_4 = -0.32 \text{ mK}$ which lead to $\alpha_1 = -5.7 \text{ mK}$ and $e_2 = 7.2 \text{ (mK)}^2$ and to a phase dia-

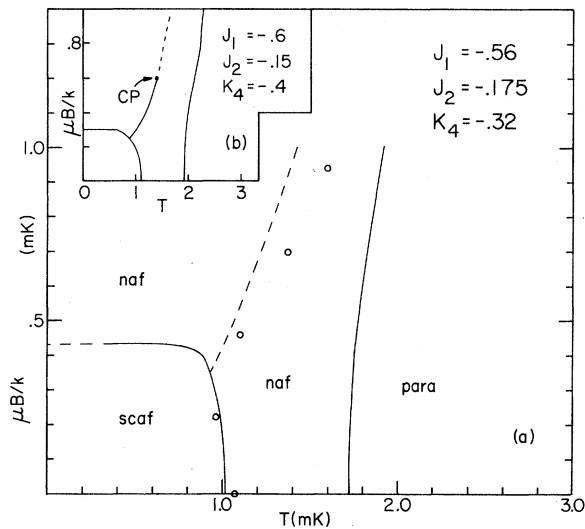


FIG. 1. (a) Phase diagram of ^3He below 3 mK as determined by experiment of Ref. 7 (open circles) and according to mean-field theory based on coefficients shown. (b) Inset shows how first-order transition with critical point (CP) can be obtained with slight adjustment of parameters.

gram as shown in Fig. 1(a). In Fig. 1(a) the experimental phase boundary from Kummer *et al.*⁷ is shown by the open circles. We find three distinct phases: To the right (above 1.8 mK) is the paramagnetic phase. Below about 1.8 mK is the naf phase. Below about 1 mK and for $\mu B/k$ below 0.45 mK is the scaf phase. The dashed line indicates a separation of the naf phase into high-entropy and low-entropy regions (taken as the line where $S/k = 0.4$). Note that the ratios of the sizes of exchange (two-atom:three-atom:P:F) used to obtain this fit conflict with present theoretical calculations.⁹⁻¹¹

Figure 2 shows the entropy as a function of temperature at various magnetic fields, which should be compared to Fig. 2 of Kummer *et al.* Note that along the upper "phase" line of Fig. 1 we do not have a discontinuity in S as a function of T but, in exact accord with Kummer *et al.*, we find a rapid entropy change which becomes smoother at higher field. The physical reason for such a rapid entropy change without an actual phase transition became apparent when the parameters were adjusted slightly away from a good fit to the high- T data and a phase diagram like that in Fig. 1(b) was obtained. In this case we find an actual first-order transition which ends in a critical point. Examination of the naf phase in the case in Fig. 1(a) "under" the scaf

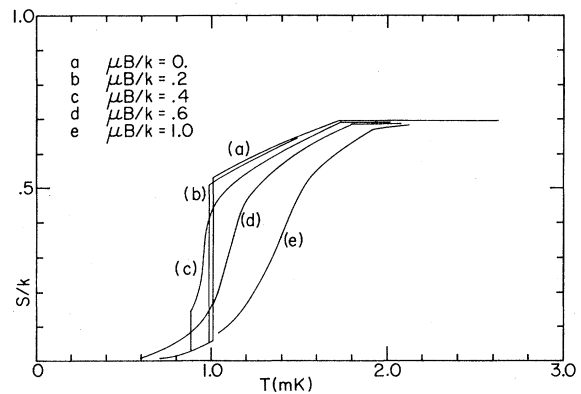


FIG. 2. Entropy versus temperature at several magnetic fields. This figure should be compared to Fig. 2 of Ref. 7.

region shows that a critical point also occurs in this case but it is "hidden" by the lower-free-energy scaf phase.

Taking a hopeful stance we might identify the naf-paramagnetic transition with the bump in specific heat near 2 mK noticed by Dundon and Goodkind,³ Halperin *et al.*,⁸ and Kummer *et al.*⁷ In the eventuality that such identification cannot be made we know that the naf-paramagnetic transition temperature is rather sensitive to improvements in the calculation beyond mean field. We hypothesize, however, that the scaf-naf boundary would be less affected because an examination of the variation of free energy with temperature shows that a small relative energy shift would have a large effect on the transition temperature of the naf-paramagnetic transition while in the case of the other transitions in Fig. 1(a) the same relative free-energy shift would have a much smaller effect. We would therefore expect that the second-order paramagnetic-naf transition would move down to the region of the other transitions in Fig. 1 so that the naf region to the right of the dashed line and to the right of the scaf phase might disappear.

In conclusion we have shown that there is no problem fitting almost all available solid- ^3He magnetic data with two-, three-, and four-atom exchanges. Also we have found an amazing richness of possible behavior. The possibilities when the full B - T - P space is explored are significant because we find the phase diagram to be sensitive to parameter shifts and we imagine that the ratios of the presumed physical exchanges should change under pressure.

Finally we would urge direct measurement of

the spin structure of the various phases if at all possible. We note that if our phase diagram is not correct even spiral¹⁷ or more complicated phases are not out of the question. We would also urge a more careful experimental examination of the region near the bottom of the dashed phase line to determine if an actual critical point exists.

¹M. F. Panczyk and E. D. Adams, Phys. Rev. **187**, 321 (1969).

²M. F. Panczyk and E. D. Adams, Phys. Rev. A **1**, 1356 (1970).

³J. M. Dundon and J. M. Goodkind, Phys. Rev. Lett. **32**, 1343 (1974).

⁴T. P. Bernat and H. D. Cohen, Phys. Rev. A **7**, 1709 (1973).

⁵W. P. Kirk, E. B. Osgood, and M. Garber, Phys. Rev. Lett. **23**, 833 (1969).

⁶S. B. Trickey, W. P. Kirk, and E. D. Adams, Rev. Mod. Phys. **44**, 668 (1972).

⁷R. B. Kummer, E. D. Adams, W. P. Kirk, A. S. Greenberg, R. M. Mueller, C. V. Britton, and D. M. Lee, Phys. Rev. Lett. **34**, 517 (1975).

⁸W. P. Halperin, C. N. Archie, F. B. Rasmussen, R. A. Buhrman, and R. C. Richardson, Phys. Rev. Lett. **32**, 927 (1974).

⁹A. K. McMahan, J. Low Temp. Phys. **8**, 115 (1972).

¹⁰L. I. Zane, J. Low Temp. Phys. **9**, 219 (1972).

¹¹A. K. McMahan and J. W. Wilkins, Phys. Rev. Lett. **35**, 376 (1975).

¹²A concise method of derivation is given by W. J. Mullin, Phys. Rev. B. (to be published).

¹³G. A. Baker, Jr., H. E. Gilbert, J. Eve, and G. S. Rushbrooke, Phys. Rev. **164**, 800 (1967).

¹⁴W. P. Kirk and E. D. Adams, Phys. Rev. Lett. **27**, 392 (1971).

¹⁵L. Goldstein, Phys. Rev. A **8**, 2160 (1973).

¹⁶R. A. Guyer, Phys. Rev. A **9**, 1452 (1974).

¹⁷T. A. Kaplan, Phys. Rev. **116**, 888 (1959).

Neutron-Inelastic-Scattering Measurements of Phonon Perturbations by Defects in Irradiated Copper*

R. M. Nicklow, R. R. Coltman, F. W. Young, Jr., and R. F. Wood
Solid State Division, Oak Ridge National Laboratory, Oak Ridge, Tennessee 37830
(Received 28 July 1975)

Neutron-scattering measurements have been made at 10 K of phonons in a copper crystal neutron-irradiated at 4 K. The results, though clearly showing q -dependent defect-phonon perturbation effects, could not be explained entirely by simplified calculations for the $\langle 100 \rangle$ split interstitial. A 300-K anneal removed the irradiation-induced line broadening and frequency shifts but only $\sim 50\%$ of the additional peak structure, which was completely removed only after an 800-K anneal.

It is well established that the irradiation of crystals at very low temperatures produces vacancies and interstitials, and extensive research has been focused on determining the stable structure of self-interstitials, particularly in fcc metals. Recent theoretical studies have predicted that the $\langle 100 \rangle$ dumbbell configuration is the stable form for the interstitial in Cu¹ and this has been corroborated by diffuse x-ray² and elastic-constant measurements.³ The theoretical work predicted that the dumbbell interstitial possesses low-frequency librational modes.¹ Wood and Mostoller⁴ and Schober, Tewary, and Dederichs⁵ have shown that these can undergo strong resonant hybridization with the phonons of the host crystal, which possibly could be detected by neutron scattering even for very low concentrations ($\ll 1\%$) as in the somewhat analogous case of KCl:CN⁻ recently studied by Walton, Mook,

and Nicklow.⁶ The direct observation of such resonant modes would provide new information about the structure of the interstitial, its dynamical properties, and the interatomic forces which couple it to the lattice.

Here we report the first results of neutron-coherent-inelastic-scattering experiments on perturbed phonons in a neutron-irradiated crystal. The experiment was carried out on a high-purity, low-dislocation-density crystal of dimensions $0.6 \times 1.8 \times 3.8$ cm³, with the $[1\bar{1}0]$ direction parallel to the longest dimension. The crystal was irradiated by thermal neutrons at 4.2 K for 24 days in the low-temperature facility at Oak Ridge National Laboratory.⁷ The concentration of Frenkel pairs was ≈ 40 ppm randomly dispersed through the crystal. After irradiation the sample was transferred at 4.2 K to a liquid-helium cryostat on the triple-axis spectrometer at the